Molecular Dynamics Simulations of Gly-12→Val Mutant of p21^{ras}: Dynamic Inhibition Mechanism

Noriyuki Futatsugi* and Minoru Tsuda†

*Computational Science Division, Institute of Physical and Chemical Research, Wako-shi, Saitama 351-0198 and †Laboratory of Physical Chemistry, Faculty of Pharmaceutical Sciences, Chiba University, Chiba 263-8522, Japan

ABSTRACT The mutant p21^{ras} protein is a G protein produced by the point-mutated H-*ras* gene, and this mutant protein has been shown to cause carcinogenesis due to a reduction in its GTPase activity. However, the mechanism underlying this strange phenomenon has still not been elucidated. In our previous study, we have clarified the mechanism of the GTP→GDP hydrolysis reaction in the wild-type p21^{ras} at the atomic level and concluded that GTPase-activating protein plays a significant role in the supply of H_2O molecules for the hydrolysis. The structure of the active site in the mutant is the same as that in the wild type. However, by performing molecular dynamic calculations, we found that the structure of the active site of the enzyme substrate complex in the oncogenic mutant p21^{ras} continuously changes, and these continuous changes in the active site would make it difficult for the GTP→GDP hydrolysis reaction to occur in the mutant. These findings can explain the fact that the GTPase activity in the mutant was only 15% of that in the wild type and the fact that GTPase-activating protein has no reaction-activating effect in the mutant. This is a dynamic inhibition mechanism of a vital reaction that can be explained by considering the molecular dynamics.

INTRODUCTION

The c-Ha-*ras* gene (Shih et al., 1979) produces the small GTP-binding protein p21^{ras}. p21^{ras} is thought to play an important role in intracellular signal cascades in mammals. It has also been shown that p21^{ras}, which is a G protein, is active when GTP is bound to it but becomes inactive when GTP is hydrolyzed to GDP and inorganic phosphoric acid (Maegley et al., 1996). This transformation from being active with GTP to inactive with GDP is the molecular switching mechanism of p21^{ras} (Barbacid, 1987; Lim et al., 1996; Milburn et al., 1990).

It is known that carcinogenesis is caused by the mutant p21^{ras} substituting only an amino acid Gly-12 in the wild type to another amino acid, such as Val-12 (except Pro-12) coded by the mutant *ras* gene, or, in other words, the *ras* oncogene. It has also been experimentally shown that GTPase activity in p21^{ras} is reduced by the same substitution of Gly12 by other amino acids (except Pro-12) (Chung et al., 1993). Unless GTP→GDP hydrolysis occurs regularly, most of the p21^{ras} protein retains active conformation with GTP. The cause of carcinogenesis is thought to be an excessive induction of intracellular signal cascades due to an undesirable increase of the active conformation (Barbacid, 1987).

Because the difference between the wild-type p21^{ras} and the oncogenic mutant p21^{ras} originates from the capability of GTP→GDP hydrolysis, we investigated the mechanism by which GTP→GDP hydrolysis occurs in the wild-type p21^{ras}.

It was found, using ab initio calculations, that the proton relay reaction via ζ-nitrogen of the side chain of Lys-16 (Lys-16-N) played an important role in the mechanism of hydrolysis (Futatsugi et al., 1997, 1999). Details are shown in Fig. 1. However the amino acid (position 12) that caused carcinogenesis is not included in the structure of the active site for the proton relay via Lys-16. Therefore, molecular dynamics calculations were performed on the wild-type p21^{ras}, the Gly-12→Val oncogenic mutant p21^{ras}, and the Gly-12→Pro nononcogenic mutant p21^{ras}.

MATERIALS AND METHODS

AMBER with high-speed accelerator

MD simulations were performed on Sun SparkStation5 with the hardware accelerator called MD-Engine (Toyoda et al., 1995, 1999), using the AMBER version 4.0 software package from University of California at San Francisco (Pearlman et al., 1995).

The MD-Engine is able to calculate nonboned interactions at high speed, such as Coulomb or van der Waals interactions. Therefore, this hardware can calculate without cutoff technique, which produced some errors in the results of MD simulations and can restrain artificial behavior by errors.

Minimization and molecular dynamics

The structural model of the wild-type p21^{ras} is 121p in the protein data bank (Abola et al., 1987) data, using the nonhydrolyzed analog (guanosine-5′-[β,γ-methylene] triphosphate) in place of the GTP. The MD simulation software package AMBER was used for calculations, using the parm94 force field (Cornel et al., 1995). We created the force field and charges for GTP and Mg^{2+} in p21^{ras} using Gaussian 94 (Frisch et al., 1995a,b). Calculations were performed in the Hartree-Fock level, using a basis functional set, 6-31G**. The structures of GTP and Mg^{2+} were optimized

Received for publication 28 December 2000 and in final form 20 September 2001.

Address reprint requests to Dr. Noriyuki Futatsugi, Computational Science Division, Institute of Physical and Chemical Research (RIKEN), 2–1 Hirosawa, Wako-shi, Saitama 351-0198, Japan. Tel.: 81-48-467-9415; Fax: 81-48-467-4078; E-mail: foota@gsc.riken.go.jp.

0006-3495/01/12/3483/06 $2.00

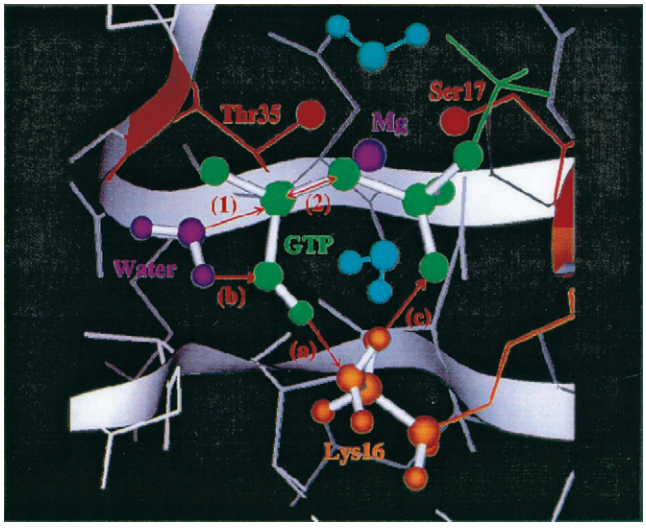

FIGURE 1 GTP→GDP hydrolysis reaction in the wild-type p21^{ras}. First, a water molecule coordinates to γ-phosphate (*1*). Next, a proton binding to the oxygen of γ-phosphate moves to Lys-16-N (*a*), and a proton of the water molecule moves to the oxygen of γ-phosphate (*b*). Next, another proton of Lys-16-N moves to the oxygen of β-phosphate (*c*), and the bond distance between γ-phosphate and β-phosphate is extended (*2*). Eventually, GTP is dissociated into GDP and a phosphate.

and decided charges in atoms and then the force field was produced using these charges by the PREP program in the AMBER.

To mimic aqueous solvent conditions, ~2800 solvent water molecules (TIP3P water model) were created using the Monte Carlo method, as the whole enzyme was enveloped by a water layer of 30 Å in radius. The whole structure including solvent waters was energy minimized.

First, the temperature was gradually increased to 300 K for 104 ps, and then the kinetic energy for MD simulation was provided by a thermal bath at a constant temperature required for vital body conditions, 300 to 310 K, for 1000 ps (5000 steps of 2.0 fs each) using SHAKE method. Nonbonded interactions were evaluated without a cutoff distance using the MD-Engine. The simulation outputted data occurring every 100 fs during the trajectory and stored as a history file. The oncogenic mutant (Gly-12-Val; 521p) (Pai et al., 1989, 1990) and the nononcogenic mutant (Gly-12-Pro; 821p) (Krengel et al., 1990; Scheidig et al., 1992; Pai et al., 1990) were also calculated by the same procedure as that used for the wild-type p21^{ras}.

RESULTS AND DISCUSSION

Dynamic inhibition mechanism

The results showed that there is a clear difference in terms of time between the structures of the active sites of the wild type and mutants. The following is explanation for the results using figures and these picked up structures at 700 ps with clear differences between the wild type and mutants. Fig. 2 shows the changes in function time in the structure of the active site of the wild-type p21^{ras} and, as one example, the structure of the active site of the wild type at 700 ps. As can be seen in these figures, the active site of the wild-type p21^{ras} maintains a regular structure with few changes. However, the oncogenic mutant p21^{ras} showed quite different changes in function time in its structure. Fig. 3 shows changes in function time in the structure of the Gly-12→Val oncogenic mutant p21^{ras} and one example of the structure of this mutant. The results for the Gly-12→Pro nononcogenic mutant p21^{ras} are shown in Fig. 4. Certainly,

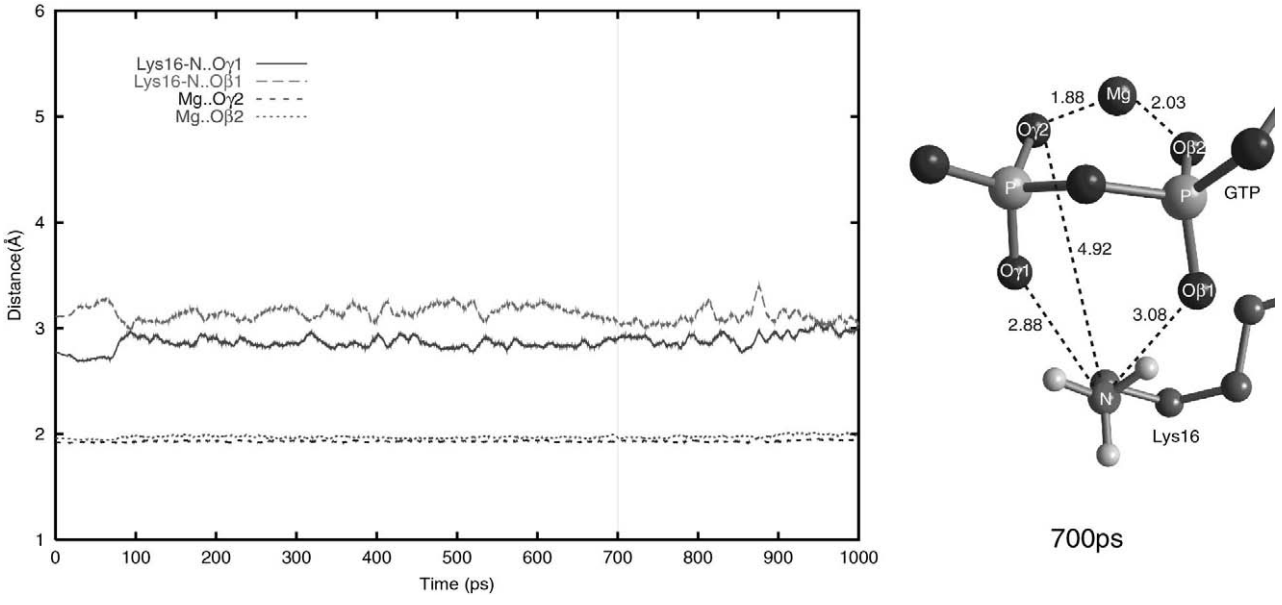

FIGURE 2 Results of molecular dynamics calculation for the wild-type p21^{ras}. The abscissa indicates time (ps) for molecular dynamics, and the ordinate indicates distances (Å) among atoms in the active site of p21^{ras}. Both the distances between Lys-16-N and the oxygen of γ-phosphate (N-Oγ1) and between Lys-16-N and the oxygen of β-phosphate (N-Oβ1) remain constant at ~3 Å. The distances between Mg and the oxygen of γ-phosphate (Mg-Oγ2) and between Mg and the oxygen of β-phosphate (Mg-Oβ2) also remain constant at ~2 Å. The structure shown is an example of the wild-type p21^{ras} at 700 ps (Å).

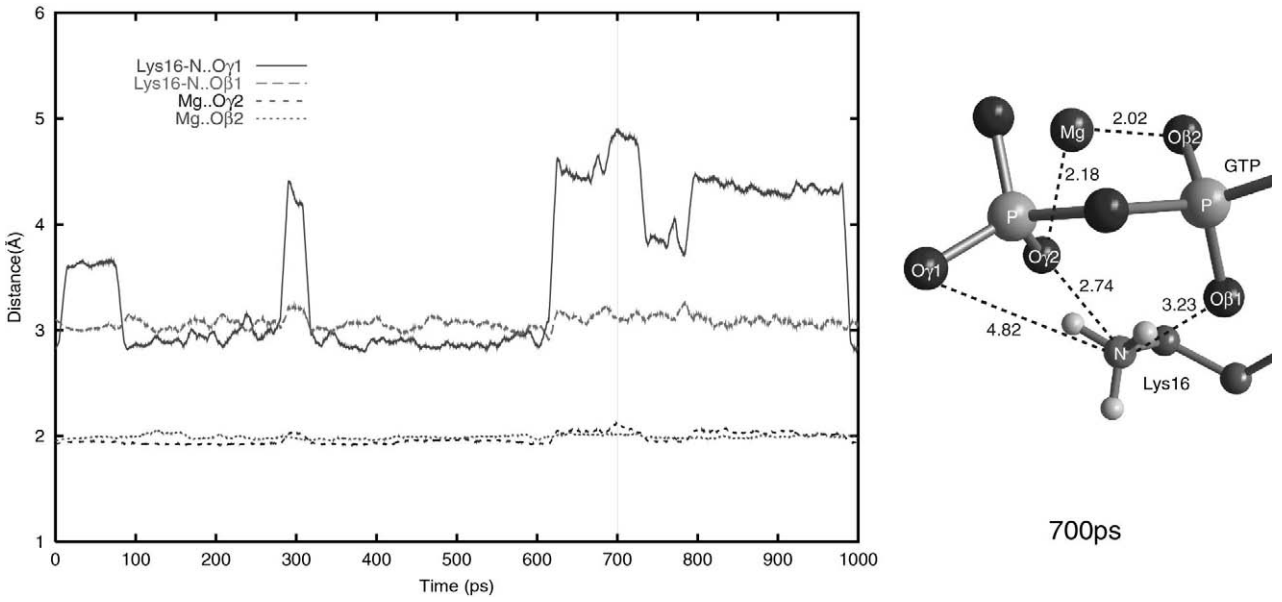

FIGURE 3 Results of molecular dynamics calculation for the Gly-12→Val oncogenic mutant p21^{ras}. The abscissa indicates time (ps) for molecular dynamics and the ordinate indicates distances (Å) among atoms in the active site of p21^{ras}. The distance between Lys-16-N and the oxygen of β-phosphate (N-Oβ1) remains at ~3 Å, but the distance between Lys-16-N and the oxygen of γ-phosphate (N-Oγ1) fluctuates irregularly. Mg holds GTP as it does in the wild-type p21^{ras}. The structure shown is an example of the Gly12→Val oncogenic mutant p21^{ras} at 700 ps (Å). The distance between Lys-16-N and the oxygen of γ-phosphate (N-Oγ1) has been expanded from 2.88 Å in the normal structure (Fig. 2) to 4.82 Å, and Lys-16-N approaches the oxygen coordinating to Mg instead of the oxygen of γ-phosphate (Oγ2) (4.92 Å → 2.74 Å).

it seems that the nononcogenic mutant fulfills its mechanism in the same manner as does the wild type, because changes in function time in the active site structure of the nononcogenic mutant are very similar to those in the wild type. According to these figures, the distance between Lys-16-N and γ-phosphate in the oncogenic mutant p21^{ras} fluctuates between ~3 and 5 Å, thereby changing the active structure for hydrolysis of the enzyme.

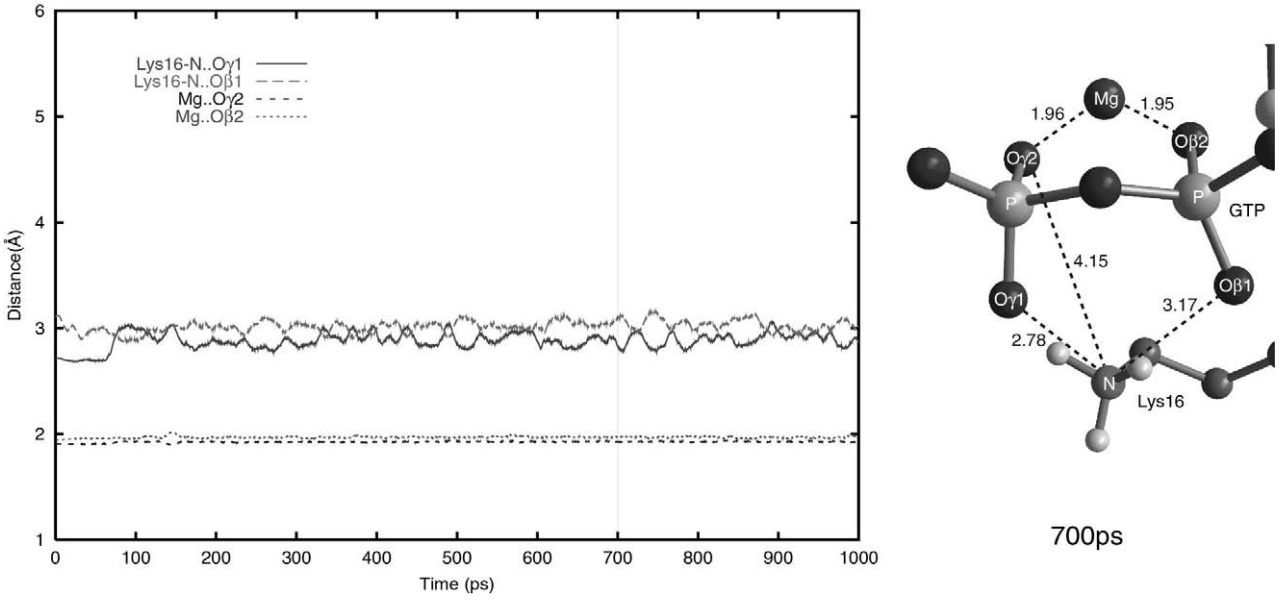

FIGURE 4 Results of molecular dynamics calculation for the Gly-12→Pro nononcogenic mutant p21^{ras}. The abscissa indicates time (ps) for molecular dynamics and the ordinate indicates distances (Å) among atoms in the active site of p21^{ras}. These results are very similar to those for the wild type. The structure shown is an example of the Gly-12→Pro nononcogenic mutant p21^{ras} at 700 ps (Å).

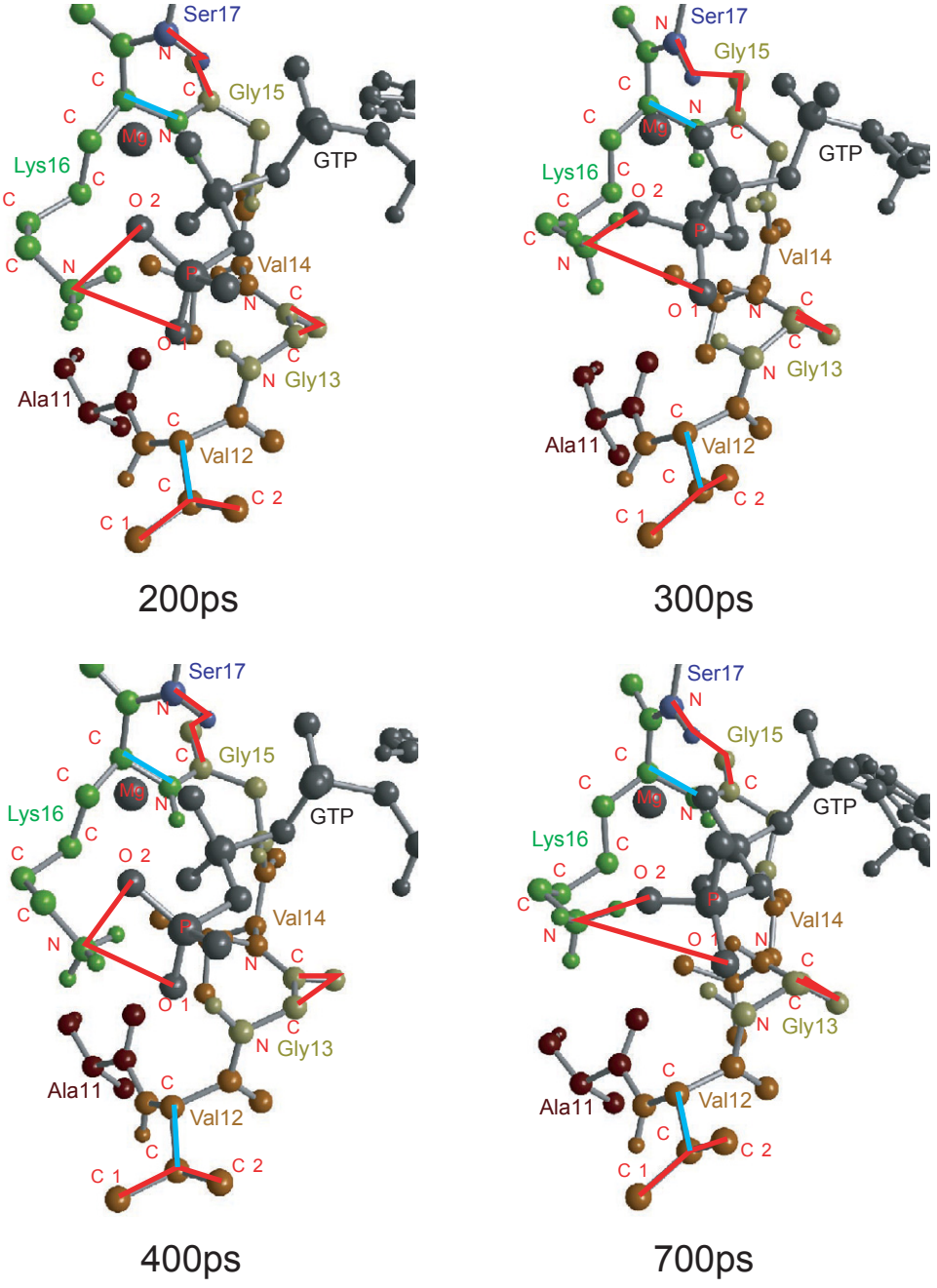

FIGURE 5 In the Gly-12→Val mutant p21^{ras}, the structures at: 200 ps (normal), 300 ps (change), 400 ps (normal), and 700 ps (change) are shown. The relative position between the side chain of Val-12 (Cα-Cβ) and the main chain of Lys-16 (Cα-N) (*light blue lines*) is shown with dihedral angles: 87.6° at 200 ps and 81.9° at 400 ps in the normal period, but 133.9° at 300 ps and 117.7° at 700 ps in the period of change. The side chain of Val-12 rotated perpendicularly to the loop structure constructed with the main chain of the peptide and the side chain of Lys-16. Consequently, the distance between the nitrogen of the side chain of Lys-16 (Nζ) and the oxygen of γ-phosphate (Oγ1) maintains a hydrogen bond in the normal period but extends in the period of change and Nζ of Lys-16 exchange the bond with Oγ2 of γ-phosphate instead of Oγ1. The structural differences among the structures in the normal period and the period of change are shown by red lines; i.e., the direction of the side chain of Val-12 (Cγ1-Cβ-Cγ2), the positions of C and Cα of the main chain of Val-13, and the relative positions between C of Gly-15 and N of Ser-17 were confirmed.

Thus, the spatial position of Lys-16 in the active site of the oncogenic mutant p21^{ras} is unstable, and the active site structure of enzyme substrate (ES) complex is broken and later restored. This suggests that the GTP→GDP hydrolysis reaction shown in Fig. 1 rarely occurs in the oncogenic mutant p21^{ras}. The GTPase activity in the Gly-12→Val mutant p21^{ras} remains at ~15% (Chung et al., 1993) because, as shown in Fig. 3, the proton relay reaction occurs

while the hydrogen bond between Lys-16-N and the oxygen of γ-phosphate is kept at a distance of ~3 Å.

Because the crystal structure of the ES complex of the Gly-12→Val mutant p21^{ras} determined by x-ray analysis is not different from that of the wild-type p21^{ras}, this blocking mechanism of enzyme activity was determined by molecular dynamics. For this reason, this blocking mechanism could be termed a "dynamic inhibition mechanism."

The GTP hydrolysis ability of p21^{ras} is enhanced by creating a complex with Ras-GTPase-activating protein (p120-GAP) (Ahmadian et al., 1997; Boguski and McCormick, 1993; Giglione et al., 1997) and the Gly-12→Val oncogenic mutant p21^{ras} binds to GTPase-activating protein (GAP) with an affinity similar to that of the wild type (Gideon et al., 1992). However, GAP-accelerated GTP hydrolysis is blocked in the case of the Gly-12→Val mutant p21^{ras}. Scheffzek et al. (1997) analyzed the crystal structure of the Ras-RasGAP complex and discussed the effect of the mutation of residue 12, and then they described "the closest encounter being a van der Waals contact between the Cα atom of Gly-12 and the mode of interaction imposes constraints on the space that may be filled by amino acids in position 12 of Ras and provides an explanation for the block in GAP-accelerated GTP hydrolysis." However we consider that reduction of GTPase activity have other main origin of the blocking involved directly reaction in the active site, and this is not able to be seen on the static x-ray crystal structure. The Gly-12→Val oncogenic mutant p21^{ras} has a similar structure in the active site to that of the wild type and the Gly-12→Pro nononcogenic mutant, and the crystal structures are almost the same. Thus, the difference in action between the wild type and the Gly-12 mutant p21^{ras} cannot be found by studying only the static structures. In the present study, we showed, using a dynamic method, that there are changes in function time in the active site originating from the substitution of Gly-12 by another amino acid, and we succeeded to clarify the origin of the carcinogenesis caused by a point mutation.

How does the dynamic inhibition mechanism operate?

Fig. 5 shows the structures determined by MD calculations at 200 ps (normal), 300 ps (change), 400 ps (normal), and 700 ps (change), respectively, in the Gly-12→Val mutant p21^{ras}. "Normal" means that the structure of the active site keeps a hydrogen bond between the Lys-16-N and the oxygen of the γ-phosphate. "Change" means the structure of the active site does not keep a hydrogen bond. To clarify the characteristics of the structures, the main chain of the peptide with the side chain of Lys-16 is shown in each of the four structures in Fig. 6. It is clear from Fig. 6 that the structures at 200 ps and the 400 ps in the normal period, as well as structures at 300 ps and the 700 ps in the period of change are very similar in each group, but the structures between these two groups are very different. To investigate

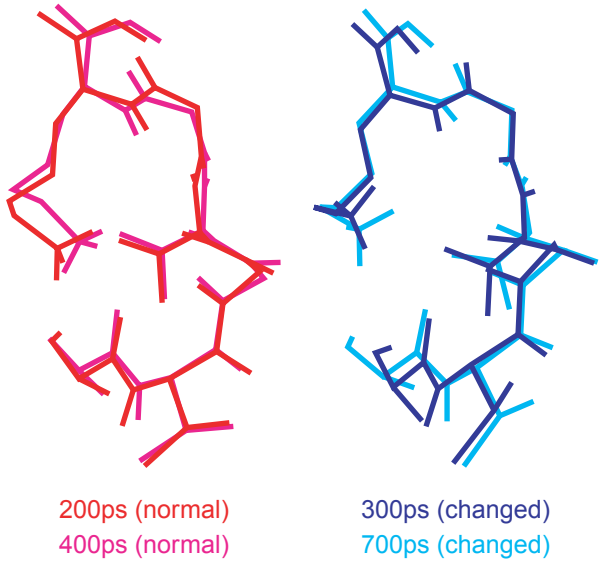

FIGURE 6 In the Gly-12→Val mutant p21^{ras}, the structures at 200 ps (*red*) and 400 ps (*pink*) in the normal period as well as the structures at 300 ps (*blue*) and 700 ps (*light blue*) in the period of change are very similar in each group for Ala-11 through Ser-17 in the loop structure, but structures between these two groups are very different.

the origin of the difference, the relative position between the Cα-Cβ bond of the side chain of Val-12 and the Cα-N bond of the main chain of Lys-16 (light blue lines in Fig. 5) was measured with respect to the dihedral angles, and large differences in angle were found among these structures in the normal period and the period of change; i.e., 87.6° at 200 ps and 81.9° at 400 ps in the normal period, on the other hand, 133.9° at 300 ps and 117.7° at 700 ps in the period of change. This result shows that the side chain of Val-12 rotates perpendicularly with respect to the plane of the loop structure constructed with Ala-11, Val-12, Gly-13, Val-14, Gly-15, and Lys-16. Consequently, the relative positions of C and Cα (red line in Fig. 5) of Gly-13 were different in the two groups; i.e., Cα turned down to the position of C in the normal period but turned up to C at almost the same height in the period of change. In addition to this change, we found that the positions between Gly-15 and Ser-17 (red line in Fig. 5) were different across the main chain of Lys-16 in the period of change as compared with the structures in the normal period. On the structure of Lys-16, the positions of Cγ, Cδ, Cε, and Nζ are very different in the two groups. For this reason, the distance between Nζ of Lys-16 and Oγ1 of γ-phosphate keeps a hydrogen bond in the normal period but no hydrogen bond in the period of change. And, the distance between Nζ of Lys-16 and Oγ2 of γ-phosphate forms a hydrogen bond in the latter. That is, because the side chain of Val-12 sways perpendicularly to the plane constructed by the main chain of the peptide and the side chain of Lys-16, this sway is the trigger to change the position of the side chain of Lys-16 to produce two kinds of

hydrogen bond; i.e., a hydrogen bond between Nζ of Lys-16 and Oγ1 of γ-phosphate or that of Nζ and Oγ2.

The wild-type p21^{ras} with Gly-12, however, differs from the case of Val-12 because Gly-12 has no side chain and does not trigger by the sway of the side chain to the loop structure constructed with the main chain of the peptide and the side chain of Lys-16. The Gly-12→Pro nononcogenic mutant p21^{ras} increases the stability of the loop structure because the circular structure of the main chain arising from Pro, which has no side chain, cannot trigger by the sway.

Therefore, we conclude that the origin of the dynamic inhibition mechanism is the instability of the position of Lys-16-N, which is brought about by the force to the main chain of the peptide caused by sway of the side chain of Val-12.

CONCLUSIONS

The stability of the spatial position of Lys-16, which plays a central role in the mechanism of the GTP→GDP hydrolysis reaction, fluctuates in the Gly-12 mutant p21^{ras}, which is created by the H-*ras* oncogene. Thus, in the wild-type and the nononcogenic mutant p21^{ras}, the structure of the active site for the GTP→GDP hydrolysis reaction remains intact under vital body conditions, but in the oncogenic mutant p21^{ras}, the distance between Lys-16-N and γ-phosphate continuously changes time after time, destroying the structure of the ES complex and thereby making it very difficult for the GTP→GDP hydrolysis reaction to occur. This demonstrates the existence of a new mechanism for dynamic inhibition of a vital reaction. The point-mutated H-*ras* acts as an oncogene by coding the Gly-12 mutant p21^{ras} with this dynamic inhibition mechanism.

This work was supported in part by the supercomputer system Fujitsu 700E vector parallel computer of the Institute of Physical and Chemical Research (RIKEN). The computations were also carried out by the DRIA System at the Faculty of Pharmaceutical Sciences, Chiba University.

REFERENCES

Abola, E. E., F. C. Bernstein, S. H. Bryant, T. F. Koetzle, and J. Weng. 1987. Protein data bank. *In* Crystallographic Databases: Information Content, Software Systems, Scientific Applications. Data Commission of the International Union of Crystallography, Bonn/Cambridge/Chester. 107–132.

Ahmadian, M. R., R. Mittal, A. Hall, and A. Wittinghofer. 1997. Aluminium fluoride associates with the small guanine nucleotide binding proteins. *FEBS Lett.* 408:315–318.

Barbacid, M. 1987. ras gene. *Ann. Rev. Biochem.* 56:779–827.

Boguski, M. S., and F. McCormick. 1993. Proteins regulating Ras and its relatives. *Nature.* 366:643–654.

Chung, H.-H., D. R. Benson, and P. G. Schultz. 1993. Probing the structure and mechanism of Ras protein with an expanded genetic code. *Science.* 259:806–809.

Cornel, W. D., P. Cieplak, C. I. Bayly, I. R. Gould, K. M. Merz, Jr., D. M. Ferguson, D. C. Spellmeyer, T. Fox, W. Caldwell, and P. A. Kollman. 1995. A second generation force field for the simulation of proteins, nucleic acids and organic molecules. *J. Am. Chem. Soc.* 117:5179–5197.

Frisch, M. J., Æ. Frisch, and J. B. Foresman. 1995a. Gaussian94 User's Reference. Gaussian, Inc.

Frisch, M. J., Æ. Frisch, and J. B. Foresman. 1995b. Gaussian94 Programmer's Reference. Gaussian, Inc.

Futatsugi, N., M. Hata, T. Hoshino, and M. Tsuda. 1997. The importance of the role of lysine 16 and GAP on the molecular switching mechanism of Ras protein p21. *J. Chem. Soc. Jpn.* 7:516–522.

Futatsugi, N., M. Hata, T. Hoshino, and M. Tsuda. 1999. Ab initio study of the role of lysine 16 for the molecular switching mechanism of Ras protein p21. *Biophys. J.* 77:3287–3292.

Gideon, P., J. John, M. Frech, A. Lautwein, R. Clark, J. E. Scheffler, and A. Wittinghofer. 1992. Mutational and kinetic analyses of the GTPase-activating protein (GAP)-p21 interaction: the C-terminal domain of GAP is not sufficient for full activity. *Mol. Cell. Biol.* 12:2050–2056.

Giglione, C., M. C. Parrini, S. Baouz, A. Bernardi, and A. Parmeggiani. 1997. A new function of p120-GTPase-activating protein. *J. Biol. Chem.* 272:25128–25134.

Krengel, U., I. Schlichting, A. Scheidig, M. Frech, J. John, A. Lautwein, F. Wittinghofer, W. Kabsch, and E. F. Pai. 1991. The three-dimensional structure of p21 in analysis of oncogenic mutants. *N.A.T.O. A.S.I. Ser. Ser. A.* 220:183–193.

Krengel, U., I. Schlichting, A. Scherer, R. Schumann, M. Frech, J. John, W. Kabsch, E. F. Pai, and A. Wittinghofer. 1990. Three-dimensional structures of H-ras p21 mutants: molecular basis for their inability to function as signal switch molecules. *Cell.* 62:539–548.

Lim, L., E. Manser, T. Leung, and C. Hall. 1996. Regulation of phosphorylation pathways by p21 GTPases the p21 Ras-related Rho subfamily and its role in phosphorylation signalling pathways. *Eur. J. Biochem.* 272:171–185.

Maegley, K. A., S. J. Admiraal, and D. Hershlag. 1996. Ras-catalyzed hydrolysis of GTP: a new perspective from model studies. *Proc. Natl. Acad. Sci. U.S.A.* 93:8160–8166.

Milburn, M. V., L. Tong, A. M. DeVos, A. Brunger, Z. Yamaizumi, S. Nishimura, and S.-H. Kim. 1990. Molecular switching for signal transduction: structural differences between active and inactive forms of protooncogenic ras proteins. *Science.* 247:939–945.

Pai, E. F., W. Kabsch, U. Krengel, K. C. Holmes, J. John, and A. Wittinghofer. 1989. Structure of the guanine-nucleotide-binding domain of the Ha-*ras* oncogene product p21 in the triphosphate. *Nature.* 341: 209–214.

Pai, E. F., U. Krengel, G. A. Petsko, R. S. Goody, W. Kabsch, and A. Wittinghofer. 1990. Refined crystal structure of the triphosphate conformation of H-ras p21 at 1.53 Å resolution: implications for the mechanism of GTP hydrolysis. *EMBO J.* 9:2351–2359.

Pearlman, D. A., D. A. Case, J. W. Caldwell, W. S. Ross, T. E. Cheatham, I. I. I., D. M. Ferguson, G. L. Seibel, C. Singh, and P. A. Kollman. 1995. AMBER Version 4.1. University of California, San Francisco, CA.

Scheffzek, K., M. R. Ahmadian, W. Kabsch, L. Wiesmuller, A. Lautwein, F. Schmitz, and A. Wittinghofer. 1997. The Ras-RasGAP complex: structural basis for GTPase activation and its loss in oncogenic Ras mutants. *Science.* 277:333–338.

Scheidig, A. J., E. F. Pai, I. Schlichting, J. Corrie, G. P. Reid, A. Wittinghofer, and R. S. Goody. 1992. Time-resolved crystallography on H-ras p21. *Phil. Trans. Roy. Soc. Lond. A.* 340:263–272.

Shih, C., B. Shilo, M. P. Goldfarb, A. Dannenberg, and R. A. Weinberg. 1979. Passage of phenotype of chemically transformed cells via transfection of DNA and chromatin. *Proc. Natl. Acad. Sci. U.S.A.* 76: 5714–5718.

Toyoda, S., E. Hashimoto, H. Ikeda, and N. Miyakawa. 1995. Development of a high speed special-purpose parallel processor system for molecular dynamics. *Tech. Rep.* 10.

Toyoda, S., H. Miyagawa, K. Kitamura, T. Amisaki, E. Hashimoto, H. Ikeda, A. Kusumi, and N. Miyakawa. 1999. Development of MD engine: high-speed accelerator with parallel processor design for molecular dynamics simulations. *J. Comput. Chem.* 20:185–199.